Optical and Quantum Electronics (2004) 36:1275–1281
DOI 10.1007/s11082-005-10317-2

Ultra-compact multimode interference InGaAsP multiple quantum well modulator

D.A. MAY-ARRIOJA[1,*], P. LIKAMWA[1], R.J. SELVAS-AGUILAR[2] AND J.J. SÁNCHEZ-MONDRAGÓN[3]
[1]*College of Optics and Photonics: CREOL & FPCE, University of Central Florida, Orlando, FL 32816, USA*
[2]*Centro de Investigaciones en Optica, Lomas del Bosque 115, León, Gto. 37150, México*
[3]*Instituto Nacional de Astrofísica, Optica y Electrónica, Apdo. Postal 51, Tonantzintla, Pue. 7200, México*
*(*author for correspondence: E-mail: may@creol.ucf.edu)*

Received 8 December 2004; accepted 7 January 2005

Abstract. We propose a new structure for an ultra-compact multimode interference (MMI) InGaAsP multiple quantum well modulator. The operating principle is based on restricting the coupling of the self-image produced by the MMI region into a single mode output waveguide. The key is to excite only the even modes within the MMI region, and this is achieved by operating the MMI waveguide under the condition of restricted symmetric interference. By asymmetrically inducing a phase change of π along a selected area within the MMI region, mode conversion of all the even modes to odd modes is achieved. Since only the fundamental mode can be coupled to the output waveguide, neither an individual mode, nor any combination of the modes will be coupled, and therefore the injected light is fully attenuated. The modulation characteristics are analyzed using the finite-difference beam propagation method. Extinction ratios as low as −37 dB are demonstrated without electro-absorption effects. For the case of low electro-absorption, which corresponds to a more realistic situation, this value is only increased to −35 dB.

Key words: integrated optics, modulator, multimode interference, multiple quantum wells, semiconductors

1. Introduction

High-speed modulators are essential components for the development of photonic integrated circuits (PICs). In particular, modulation at a wavelength of 1.55 μm is critical, since minimum dispersion and absorption occur for silica fibers around this wavelength. External modulators, such as the Mach–Zehnder (MZ) interferometer, are very attractive since they have been commercially deployed using bulk $LiNbO_3$ crystals. However, these devices are usually quite long, which is a severe limitation for the development of monolithic applications where device length reduction is essential for large-scale integration. A significant improvement has been obtained in MZ modulators employing semiconductor multiple quantum wells (MQW), because they take advantage of the larger electro-optic coefficient (Zucker *et al.* 1989) that is obtained through the quantum-confined Stark effect

(QCSE). This has provided more compact devices with lower operating voltages, and compatibility to laser/modulator integration (Rolland *et al.* 1993; Fetterman *et al.* 1996). Nevertheless, device length reduction is still limited due to the requirements of beam splitter and combiner segments, resulting in MZ modulators that are still greater than one millimeter in length (Barton *et al.* 2003).

Multimode Interference (MMI) devices, on the other hand, have drawn a great deal of interest because of their compactness, low polarization sensitivity, and relaxed fabrication tolerances. They have evolved from passive to active devices through perturbation of the refractive index within selected areas of the MMI region, leading to the realization of very compact photonic switches (Yagi *et al.* 2000; Chun-Hung *et al.* 2002). Previously, a multimode waveguide modulator/switch on $LiNbO_3$ was reported (Campbell and Li 1979). In this device, the refractive index is modified symmetrically along the longitudinal axis of the MMI region, such that the even modes will experience a larger refractive index change than the odd modes. This effectively modifies the phase difference between even and odd modes, causing the light to be switched or modulated, but requiring the use of very high voltages. Recently, Earnshaw and Allsopp (2002) reported a similar structure employing semiconductor MQW to reduce the operating voltage. However, the extinction ratio (ER) is significantly affected when the effects of absorption modulation are taken into account, even for the case of low absorption modulation. Since both modes are present in the MMI waveguide, this is mainly due to the fact that the even modes are more attenuated as compared to the odd modes.

In this paper, we propose an ultra-compact MMI-based InGaAsP MQW optical modulator. The device is relatively simple, and the key is to operate the MMI region in the regime of restricted symmetric interference for which only the even modes are excited. Therefore, by asymmetrically modifying the refractive index along a selected area within the MMI region, such that a phase change of π is induced, mode conversion of the even modes into odd modes is realized. As the output waveguide is single mode, the light can not be coupled, and the signal is efficiently modulated. The modulation characteristics are analyzed using the finite-difference beam propagation method (FD-BPM), and the analysis demonstrates an ER as low as −37 dB without absorption effects. This value increases minimally to −35 dB for the case of low absorption modulation.

2. Device structure

A schematic of the proposed MMI modulator is shown in Fig. 1(a). The device consists of a 12 μm wide and 350 μm long MMI waveguide. Light is

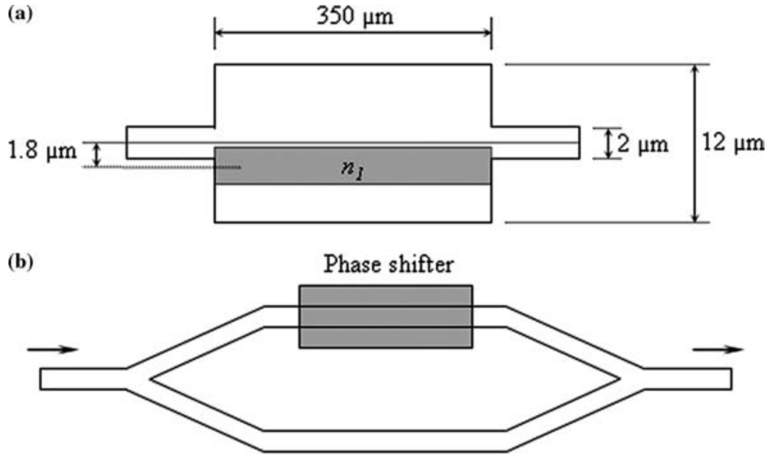

Fig. 1. (a) MMI modulator design parameters, and (b) Y-branch MZ intensity modulator.

launched and extracted from the MMI region using 2 μm wide single mode waveguides. The dimensions of the MMI region are calculated such that the injected light will be coupled to the output waveguide. The shaded area, denoted by n_1 in Fig. 1(a), indicates the index-modulated region which has a width of 3.5 μm and is shifted by a distance of 1.8 μm, measured from the center of symmetry of the device to the center of symmetry of the index-modulated region. The operational principle of the device is very similar to the Y-branch MZ modulator shown in Fig. 1(b). In the MZ modulator, light injected into the single mode input waveguide is divided into two beams. If no phase shift is applied, the beams recombine with the same phase and the light is coupled into the single mode output waveguide. However, when a π phase shift is applied to one of the arms of the MZ interferometer, the beams are recombined out-of-phase. Therefore, the electric field distribution becomes a higher-order mode and light is not coupled into the single mode output waveguide, effectively modulating the injected light.

In our device, modulation is also achieved by restricting the coupling of the light into the output waveguide, but relies on a much simpler method than the MZ modulator. The MMI modulator operates under the condition of restricted symmetric interference. In this regime, only the even modes are excited within the MMI waveguide by center-feeding the MMI region with a symmetric mode. This is achieved by injecting the light into the MMI region using a single mode input waveguide. In addition, a shorter device is obtained since the distance at which the first image will be formed is reduced by a factor of four (Soldano and Pennings 1995). When the index-modulated region is not perturbed, there is no mode conversion, and therefore an exact replica of the input beam is produced at the end of the MMI region, and subsequently coupled into the output waveguide. However, when a π phase shift is induced, as shown by the shaded region in Fig. 1(a), the phase of the propagating modes is asymmetrically-modified such that all the even modes are converted to odd modes. Since the output is a single mode waveguide, neither an individual mode nor any combination of the modes will be coupled. This allows for modulation of the propagating beam by alternately introducing and removing the applied phase shift.

3. Analysis

The FD-BPM was used to analyze the characteristics of the MMI modulator. The modeled structure consisted of a 1 μm thick, n-type, InP buffer layer. The guiding region is formed by 14 pairs of 100 Å thick, undoped, InGaAsP ($E_g = 0.816$ eV) quantum wells interspaced with 100 Å InGaAsP ($E_g = 1.08$ eV) barriers. The MQW are topped by a 1.7 μm, p-type, InP capping layer. The refractive indices of the core n_{core} and cladding n_{clad}, at a wavelength of 1.55 μm, are 3.4058 and 3.1700, respectively. The propagation characteristics without index modulation are shown in Fig. 2(a). As previously explained, the input beam propagates through the MMI region, and an exact replica of the input beam is formed at the end that couples to the

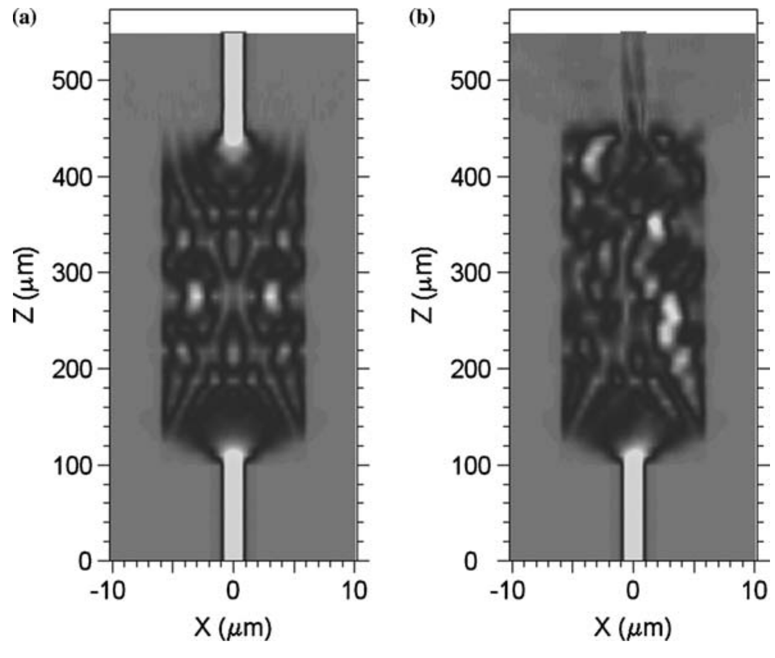

Fig. 2. Beam propagation characteristics (a) Without index modulation, and (b) With an index modulation of $\Delta n = 1 \times 10^{-2}$.

output waveguide. From the symmetry of the interference pattern, it is clear that only the even modes are propagating within the MMI structure. If coupling losses are not considered, a 0.3 dB insertion loss is calculated as a result of the imaging properties of the MMI waveguide. For the case where the index is modulated, a maximum refractive index change of $\Delta n = 1 \times 10^{-2}$ is assumed in the MQW due to the QCSE (Zucker *et al.* 1989). In order to find the optimum width and lateral position of the index-modulated region, different widths were simulated, and the lateral position was scanned from the center to the edge of the MMI waveguide. From our simulations, a width of 3.5 μm and an offset of 1.8 μm, measured from the center of symmetry of the MMI waveguide to the center of symmetry of the index-modulated region, provided the lowest ER. The propagation characteristics when this amount of index change is induced are shown in Fig. 2(b). Under these conditions, as expected, the light is not coupled to the output waveguide and the beam is fully-attenuated.

Electro-absorption effects are modeled using the ratio $\rho = \Delta n/\Delta\kappa$, where Δn and $\Delta\kappa$ are the real and imaginary parts of the complex refractive index change, respectively. This is a useful figure of merit for phase modulators because it relates the amount of index change to the induced losses. The modulator response as a function of the refractive index change (using the optimum width and offset of the index-modulating region as previously calculated) when zero absorption is considered ($\rho = \alpha$) is shown in Fig. 3.

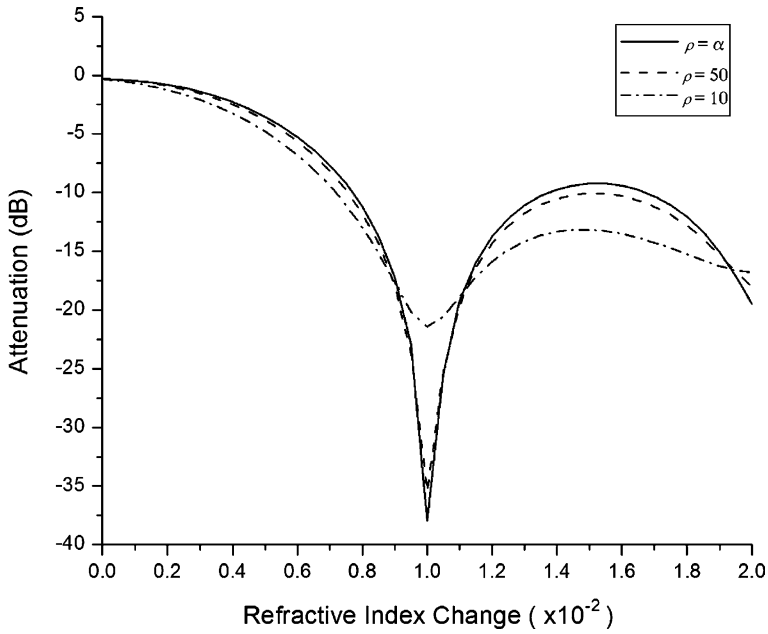

Fig. 3. MMI modulator performance as a function of the induced refractive index change.

It can be observed that an ER as low as −37 dB can be easily obtained when electro-absorption effects are not included in the simulations. As suggested by Earnshaw and Allsopp (2002), values of $\rho = 50$ and $\rho = 10$, corresponding to the cases of low and high absorption modulation respectively, were used to model the effects of electro-absorption. By using these values, a direct comparison of our device performance with other electro-refractive modulators can be obtained, since these values correspond to the upper and lower limits typically found in modulators operating by the QCSE (Chin 1992).

The characteristics of the modulator when a value of $\rho = 10$ is assumed, for the case of high absorption modulation, are also shown in Fig. 3. In this case, the ER is increased to −21 dB, which is still better when compared to typical MZ modulators operating under the same value of absorption modulation (Earnshaw and Allsopp 2002). However, when $\rho = 50$ is used in the simulations, which is a more realistic value for the case of low electro-absorption, the change in contrast ratio is almost negligible. The modulator response for this case is also shown in Fig. 3, where it can be observed that the ER increases minimally to −35 dB, as compared to an ER of −37 dB for the case of zero absorption. This minor change in ER is a result of both device operation and the MMI structure. Since the device does not operates by modal interference, slight changes in the relative amplitude between the modes have only a small effect on the modulator response. It is clear from our results that if the MQW are properly designed, such that low electro-absorption is obtained at the operating wavelength, then an ultra-compact and high contrast ratio MMI modulator is feasible utilizing the proposed structure. Furthermore, high-speed operation should be achieved with this type of modulator, since the modulation speed is only limited by the device capacitance.

4. Conclusions

A new MMI modulator structure is proposed that allows for a very compact device, while maintaining an excellent ER. The device is only 350 μm long, and has an ER of −37 dB when electro-absorption effects are not included. This value is reduced slightly to −35 dB for the case of low electro-absorption modulation. Even under the assumption of very high electro-absorption, the device should achieve an ER of −21 dB. This is a significantly better performance as compared with typical MZ modulators operating under similar electro-absorption values. The proposed MMI modulator can be easily integrated with other photonic components, and is very well suited for the development of PICs.

References

Barton, J.S., J.E. Skogen, M.L. Masanovic, S.P. Denbaars and L.A. Coldren. *IEEE J. Select. Topics in Quantum Electron* **9** 1113, 2003.
Campbell, J.C. and T. Li. *J. Appl. Phys.* **50** 6149, 1979.
Chin, M.K. *IEEE Photon. Technol. Lett.* **4** 583, 1992.
Chun-Hung, L., L. Hsueh-Hui, W. Shih-Wan, W. Hung-Jen and C. Wen-Ching. *Microwave Opt. Technol. Lett.* **33** 174, 2002.
Earnshaw, M.P. and D.W.E. Allsopp. *J. Lightwave Technol.* **20** 643, 2002.
Fetterman, M., C-P. Chao and S.R. Forrest. *IEEE Photon. Technol. Lett.* **8** 69, 1996.
Rolland, C., R.S. Moore, F. Shepherd and G. Hillier. *Electron. Lett.* **29** 471, 1993.
Soldano, L.B. and E.C.M. Pennings. *J. Lightwave Technol.* **13** 615, 1995.
Yagi, M., S. Nagai, H. Inayoshi and K. Utaka. *Electron. Lett.* **36** 533, 2000.
Zucker, J.E., I. Bar-Joseph, B.I. Miller, U. Koren and D.S. Chemla. *Appl. Phys. Lett.* **54** 10, 1989.